Pattern formation in a vibrated granular layer

Eric Clément, Loic Vanel, Jean Rajchenbach, and Jacques Duran
Laboratoire d'Acoustique et d'Optique de la Matière Condensée, URA 800 CNRS, Université Pierre et Marie Curie, B 86, 4, Place Jussieu, 75005 Paris, France
(Received 19 July 1995)

We report experiments on a vibrated bidimensional granular layer showing peak pattern formation. We measure the dispersion relation and observe two regimes of pattern selection: at low frequency, a parametric excitation of vertical shearing waves, and at high frequency, a crossover to a pattern selection with a constant wavelength. The amplitude of the patterns is proportional to the amplitude of vibration. We study the instability onset at high frequency and we find evidence of burst waves taking place in a subcritical region defined by two acceleration values.

PACS number(s): 47.54.+r, 46.10.+z, 47.20.−k, 83.70.Fn

The dynamics of noncohesive granular assemblies such as sandpiles has been an object of interest in recent years [1]. This interest is due to the rich phenomenology and the fundamental questions this system raises. In opposition to usual solids or fluids, the energy dissipation takes place at the level of granular contact (the microscopic level here) and sets this material into a new class of physical behavior. When submitted to vertical shaking, noncohesive grains show many different responses. Phenomena such as surface fluidization, convection rolls, heaping collective block motion, spatial defects, and surface waves have been reported either on three-dimensional (3D) granular systems [2–6] or in reduced dimension model media [7–10]. Recently, Melo *et al.* [11] observed, from the top of a cell in 3D, the formation of surface patterns such as stripes or squares, due to a parametric excitation of the layer, just as in experiments with fluids ([12] [13] and references therein). Note that parametric excitation studies are of fundamental importance since they constitute a unique experimental way to access directly the modes of transport of macroscopic granular assemblies and provide a crucial data set for future theoretical investigations.

Here we report on measurements performed on bidimensional layers of aluminum beads. We study in detail the dispersion relation for different layer heights and we visualize the bulk motion. We show different regimes of parametric amplification and pattern selection. We study the amplitude of the pattern and we show how it is related to the amplitude of the excitation. In the high frequency regime, we study the onset of pattern formation. Experiments in 2D of the type we present here offer a good chance for contact with ongoing computer simulation investigations.

Our experiments are made with aluminum spheres of diameter $d = 1.5$ mm. We use cells with horizontal width $L = 150$ mm and $L = 300$ mm. The cell is shaken with a vertical trajectory: $y_p(t) = a \sin \omega t$. We visualize using a charge-coupled device (CCD) video camera connected to an image processing device. The shaker operates from $f = 6$ Hz to $f = 25$ Hz with accelerations $\Gamma = a\omega^2/g$ up to $\Gamma \simeq 8$ (g is the gravitational acceleration). The normal-impact coefficient of restitution for our spheres is about $\varepsilon = 0.6$ for velocities around 1 m/s. For this dissipation parameter and for a layer of typical height at rest, $H = \sqrt{3}/2 N_h d$ (triangular piling with N_h bead layers), numerical studies indicate [14] that, for $N_h > 2$, no fluidization is expected. Note that a fluidized layer would be obtained in the limit $(1 - \varepsilon)N_h < 1$ (see [15] and reference therein), as in experiments with steel beads [10]. The relative acceleration Γ is a fundamental control parameter since theoretical studies [16] show its relevance for the response of a totally inelastic block on a vibrating plate (zeroth order description of a large assembly of inelastic particles). Experimentally, for moderate accelerations ($1 < \Gamma < 2.5$), the layer stays compacted and undergoes roughly the trajectory of a totally inelastic block. Two limiting cases of solid friction may be considered: $\mu = 0.2$ (low friction) and $\mu = 0.8$ (high friction). At this point, we note that changing the cell length and the friction coefficients did not influence noticeably the forthcoming experimental results. For beads with higher friction, convection rolls show up, generated by friction with the lateral boundaries and limited in extent to sizes of the order of N_h layers in depth. The effect of shearing by lateral boundaries has been studied elsewhere [8]. Here, we are interested in phenomena taking place far from the boundaries.

For large accelerations, a surface instability shows up as an array of peaked structures separated by a typical wavelength λ. We observe three major features.

(i) During the "free" flight (ignoring boundary effects), the amplitude of the peaks grows until the bottom plate hits the layer.

(ii) The layer is carried upwards by the plate and the peak amplitude relaxes.

(iii) The peak positions alternate i.e., a minimum corresponds to a maximum in the next period. In Fig. 1, we show two typical pictures of the peak pattern, for $N_h = 9$ beads at an acceleration $\Gamma = 3.4$. The snapshots are taken at a moment of the phase when the layer bottom hits the cell after the free flight. Figure 1(a) is obtained at an excitation frequency $f = 7.8$ Hz and Fig. 1(b) is at a higher frequency, $f = 12$ Hz. Figures 1(a) and 1(b) are rescaled since we have $\lambda_1/\lambda_2 \simeq 2$. A crucial remark here is the presence of an arching height l between the bottom of the cell and the apex of the arch. In the top view, l_1 is of the order of several tens of bead sizes and in the lower

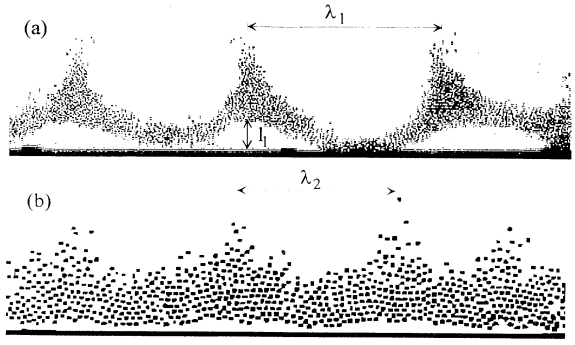

FIG. 1. Snapshot of the surface instability for $N_h = 9$ layers of beads and acceleration $\Gamma = 3.4$. The dots are the center of the beads. (a) $f = 7.8$ Hz; (b) $f = 12$ Hz. The pictures are not drawn at the same scale: $\lambda_1 = 2\lambda_2$.

view $l \simeq d$, i.e., the bead size. The value of l is decreased when the frequency is increased. In all higher frequency experiments (typically larger than 10 Hz), variations of the bottom layer position are of the order of d. Nevertheless, and for the numerous pictures we have taken, it is unclear whether we still have an arch forming or if we have merely a bottom layer random fluctuation. For a thin 3D cell, a parametric instability has been reported by Fauve *et al.* [4], showing a fingering pattern, but little quantitative information has been extracted [17]. Note that we observed similar shapes for thin layers [18]. Observation of resonant waves in small boxes has recently been reported [19]. We have studied the dispersion relation of the pattern selected for different layer heights, ranging from $N_h = 3$ to $N_h = 16$, for $7 < f < 20$ Hz. For lower value of the column height ($N_h < 3$), we do not find a clear pattern formation but rather a fluidized regime. Since the values of λ fluctuates in time, a statistical averaging is performed and is the origin of error bars that can be as large as 15%. We present in Fig. 2(a) a study of the dispersion relation for the wavelength measured, *when the peak patterns are visible.* In Fig 2(a), the wavelength λ is plotted as a function of $1/f^2$. We find a clear dependence of the wavelength on the frequency.

(i) Now let us consider the measurements made for $4 \leq N_h \leq 9$. A first set of measurements was performed with $3 < \Gamma < 4.5$. In this acceleration range, the frequency of kicks with the bottom plate is locked on the period and the free flight value is roughly one half of the period. The corresponding data of Fig. 2(b), for a given N_h, group apparently around a straight line. An important feature is a finite limiting value of λ in the asymptotic limit $f \to \infty$. We tried an empirical estimate to fit this regime and we obtained in this limited range a satisfactory agreement with an empirical law: $\lambda/\sqrt{N_h} = \lambda^*(d) + g^*/f^2$ with $\lambda^*(d) = 7.2$ mm and $g^* = 1.05$ m/s^2. Note that in 3D experiments, Melo *et al.* [11] have reported for their patterns $\lambda - \lambda_{\rm off}(d) = K(N_h)/f^2$ with a coefficient $K(N_h)$ increasing with $N_h$and saturating at larger heights. They also find an offset value depending on d. Using their empirical determination $\lambda_{\rm off}(d) = 11d$ for a layer height $H = 7d$, a remarkable agreement is obtained with our previous dispersion relation since their data would give $\lambda^*(d = 1.5\ {\rm mm}) \simeq 5.8$ mm and $g^* \simeq 1.1$ m/s^2 when used with our empirical law. Note that in view of the small range of frequencies and layer heights, the previous fit must be considered as strictly empirical since, so far, no complete theoretical account of the phenomenon has been proposed.

Alternatively, a natural idea is to consider the dispersion relation in analogy with gravity waves in fluids [20]. The dispersion relation is in this case $\omega^2 = gk\tanh(Hk)$. Note that such a relation has been recently suggested in the context of granular layers [19]. To test this idea, we plotted on the inset of Fig. 2(a) ω^2/gk as a function of Hk. Though there is a tendency for data clustering, no obvious hyperbolic tangent behavior is evidenced. Furthermore, this display shows a clear discrepancy in the

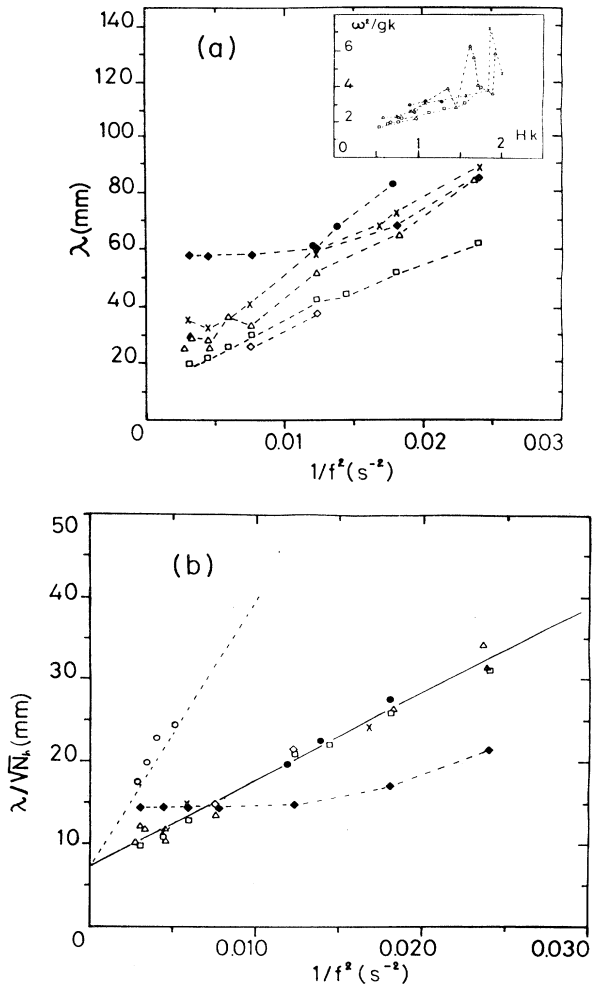

FIG. 2. Dispersion relation for $3 \leq N_h \leq 16$: $N_h = 3$ (◇); $N_h = 4$ (□); $N_h = 6$ (△); $N_h = 8$ (×); $N_h = 9$ (•); $N_h = 16$ (♦). (a) Wavelength λ as a function of $1/f^2$ for $3.3 < \Gamma < 4.2$. The inset is the scaling plot ω^2/gk as a function of Hk. (b) Rescaled wavelength $\lambda/\sqrt{N_h}$ as a function of $1/f^2$. For $3.3 < \Gamma < 4.2$, many symbols overlap; the solid line $y = 1.05x + 7.2$ is a fit. Symbol (•) is for: $\Gamma \simeq 7$ and $N_h = 9$, the dashed line is $y = 4 \times 1.05x + 7.2$. Symbols for $N_h = 16$ (♦) are connected by dashed segments as a guide to the eyes.

case of higher frequencies, corresponding to a wavelength saturation.

(ii) A natural idea emerging from Fig. 1(a), would be the existence of a growth instability of vertical shearing waves developing during the free flight trajectory of the layer. Since the shocks with the bottom plate take place at a constant pace, a specific modulation wavelength is selected and amplified parametrically. The instability is such that *the longer is the free flight, the larger is the arch amplitude l and the larger is the selected wavelength* λ. A consistency test of this qualitative interpretation scheme is provided by the response of the system when excited at higher accelerations. For $\Gamma > 6$, a transition takes place to a regime where the frequency of kicks with the bottom plate is twice as large as the period of excitation [16,3] and the free flight time is one period larger than in the previous acceleration range. Some of the resulting data points are reported in Fig. 2(b) for $N_h = 9$ (empty symbols). Obviously they do not fall on the master curve [solid line] but considering now that the effective excitation frequency is one half of the fundamental frequency, we predict those points should fall on the curve (2) which has a slope four times larger. The agreement is satisfactory.

(iii) We observe also that the high frequency saturation is not necessarily obtained in the infinite frequency limit. For instance, for $N_h = 16$ we obtain a pattern selection with a wavelength saturating at a constant value *independent of the frequency* for frequencies larger than 9 Hz. The wavelength saturation values increase with the number of layers. Apparently, there is a typical time $\tau(N, d)$ separating the two regimes. In Fig. 3, the wavelength λ is plotted as a function of Γ, for a fixed value $N_h = 16$ beads, for accelerations $\Gamma = 3$ to $\Gamma = 4.5$, and for frequencies between $f = 11$ Hz and $f = 25$ Hz. We observe that *once the pattern has developed,* the wavelength is indeed a constant: $\lambda_0 = 55 \pm 10$ mm. The fluctuations are obtained from statistical averaging for 40 snapshots.

A problem subsists for the assessment of the physics behind the wavelength high frequency saturation. Our experimental results cannot determine whether the pattern formation is produced by a remanence of the arching effect for which $l \simeq d$ or if a new phenomenon, yet to be discovered, is taking over.

Now we address the question of the pattern amplitude. In Fig 4 we report the maximum amplitude $P_{\max}$ of the

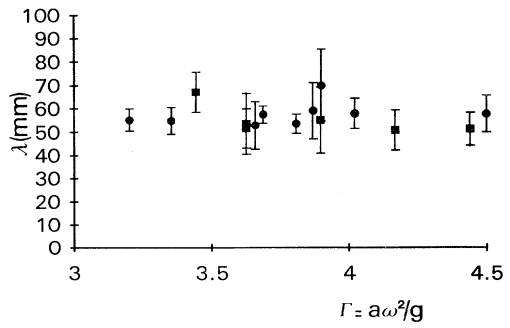

FIG. 3. Wavelength λ as a function of the acceleration Γ for $N_h = 16$: $f = 12.3$ Hz (•) and $f = 15$ Hz (■).

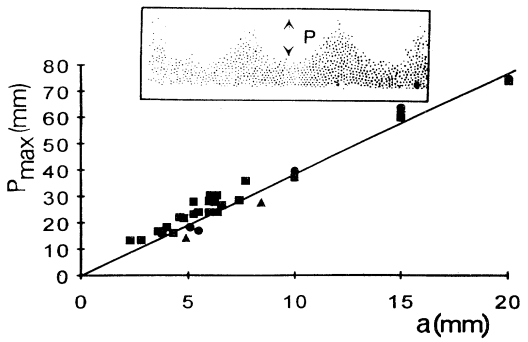

FIG. 4. Maximal amplitude of the pattern $P_{\max}$ as a function of the amplitude of excitation a, for $3.3 < \Gamma < 4.5$. The straight line is $P_{\max} = 4a$. $N_h = 6$ (+), $N_h = 9$ (•), $N_h = 11$ (▲), and $N_h = 16$ (■). The inset shows the definition of P.

peaks (obtained at the phase of contact with the bottom plate) for $3 < \Gamma < 4.2$, as a function of the amplitude of excitation. For numerous measurements, with different excitation conditions and layers of beads, a data collapse is obtained on the linear relationship $P_{\max} \simeq 4a$. A consequence is that, at constant acceleration, the phenomenon is bound to fade away at high frequency because of the finite grain size. This important result can be interpreted as follows. The peak formation is attributed to a velocity difference Δv between the zone where a peak develops and the zone where it does not. In the phase of free flight, a deformation builds up with a growing amplitude $P \sim t\Delta v$ until the impact with the bottom plate, after a free flight time $t_{\max} \sim 1/\omega$. If we estimate the velocity difference to be of the order of the impact velocity $V_{\text{impact}} \sim a\omega$, we obtain $P_{\max} \sim t_{\max}\Delta v \sim a$. This reasoning is a rough scaling estimation which does not take into account more subtle effects where the impact velocities and the times of flight may be more complicated functions of the acceleration. Also it ignores that beyond the threshold of subharmonic bifurcation ($\Gamma \simeq 3.3$), the time of free flight may vary from one period to the other. Note that the value 4 of the slope corresponds to a velocity difference of the order of $V_{\text{impact}}/2$. Data for higher amplitudes are taken in the lower frequency regime. So it seems that this interpretation is very general and that the slope value is only weakly dependent on the layer height..

Now we study the instability onset in the higher frequency regime. For a layer $N_h = 16$, we report in Fig. 5, measurements of the order parameter, i.e., the ratio $P_{\max}/a$, as a function of the relative acceleration Γ. For $\Gamma_+ > 3.2 \pm 0.1$ the regular pattern is fully developed and rather stable with $P_{\max}/a \simeq 4$. Note that this acceleration is comparable to the acceleration threshold found by Melo *et al.* in 3D (in the low frequency limit, though) and is close to the onset of the first subharmonic bifurcation for the one-inelastic-bead problem. There is a whole region between $\Gamma_- = 2.7 \pm 0.1$ and $\Gamma_+ = 3.2 \pm 0.1$ where the pattern is not stable and for which the wavelength is not well defined. We notice for the same conditions of excitation the presence of undeveloped patterns (horizontal layers), collection of uncorrelated bursts, and ultimately

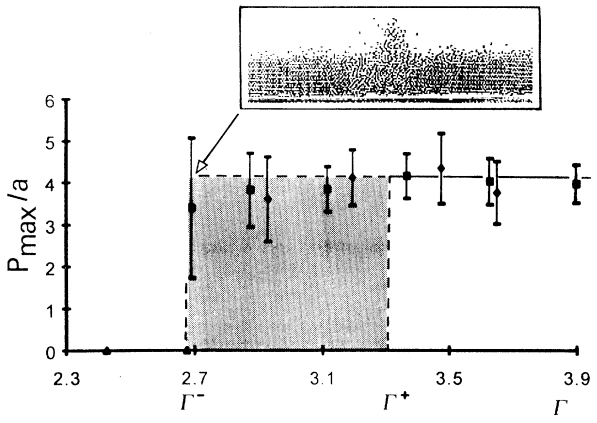

FIG. 5. Instability onset P_{max}/a as a function of the acceleration Γ: $a = 58$ mm (•) and $a = 48$ mm (♦).

we observe the intermittent occurrence of a solitary burst (see inset of Fig. 5). In this region, we also report the maximal height of all the patterns and we still find, even for the solitary burst, an average value of $P_{max}/a \simeq 4$. By varying the excitation frequency between $f = 10$ Hz and $f = 20$ Hz, we show that this threshold region is governed by the value of the relative accelerations only. The acceleration Γ_- is the lower limit for which a burst is still observed. The onset of the pattern formation has the features of subcritical bifurcation with a rather large noise amplitude. An important point is to realize that, when we reach an acceleration where a matching velocity exists between the free flight of the layer and of the vibrating plate ($\Gamma \simeq 4.5$), the phenomenon stops, and then resumes for larger acceleration ($\Gamma \simeq 6$). We are aware that in this presentation we did not discuss the influence of the subharmonic responses of the layer trajectory, spatial phase defects, the threshold dependence on the number of beads, etc. We leave these points for a more detailed presentation taking place elsewhere [18].

In this Brief Report, we report experimental measurements on a vibrated bidimensional granular layer. We study the response for different shaking accelerations and layer heights. We observe, in this geometry, a pattern formation and two regimes of pattern selection. At low frequency of excitation, we obtain a parametric excitation of vertical shearing waves with a wavelength dependent on the frequency of kicks (which can be locked on several periods of vibration of the shaker). The larger the layer free flight, the larger the vertical deformation of the layer and the larger the wavelength selected. The dispersion relation is shown to behave consistently with previous results in 3D [11]. We tested our results with respect to a simple fluid gravity wave dispersion relation and we found no clear evidence for the proof of this mechanism. For frequencies larger than a crossover value (which can be very large), we see evidence of another pattern selection scheme with a wavelength saturating at a value independent of the excitation frequency. For example, at a value of the layer as large as 16 beads, we directly probed this regime. We show that the amplitudes of the patterns are generally proportional to the amplitude of vibration. In the saturated regime, we study the instability onset and we show burst waves taking place in a subcritical region limited by two acceleration values.

We especially thank Francisco Melo, Stefan Luding, and Stefan Fauve for many interesting discussions. We acknowledge the technical assistance of Pierre Legros. LAOMC is the URA 800 of the CNRS and is part of the French Groupement de Recherche sur la Matière Hétérogène et Complexe.

[1] H.M. Jaeger and S.R. Nagel, Science **255**, 1523 (1991).
[2] P. Evesque and J. Rajchenbach, Phys. Rev. Lett. **61**, 44 (1989); P. Evesque, E. Szmatula, and J.P. Denis, Europhys. Lett. **12** , 623 (1990).
[3] S. Douady, S. Fauve, and C. Laroche, Europhys. Lett. **8**, 621 (1989).
[4] S. Fauve, S. Douady, and C. Laroche, J. Phys. (Paris) **50**, Suppl. 3, 187 (1989); S. Douady, Thèse, Ecole Normale (Paris), 1989.
[5] E.E. Ehrichs, H.M. Jaeger, G.S. Karczmar, J.B. Knight, V.Y. Kuperman, and S.R. Nagel, Science **267**, 1632 (1995).
[6] H.K. Pak and R.P. Behringer, Phys. Rev. Lett. **71**, 1832 (1993).
[7] E. Clément and J. Rajchenbach, Europhys. Lett. **16**, 133 (1991).
[8] E. Clément, J. Duran, and J. Rajchenbach, Phys. Rev. Lett. **69**, 1189 (1992); J. Duran, T. Mazozi, E. Clément, and J. Rajchenbach, Phys. Rev. E **50**, 3092 (1994).
[9] S. Luding, E. Clément, A. Blumen, J. Rajchenbach, and J. Duran, Phys. Rev. E **50**, 1634 (1994); **50**, 1762 (1994).
[10] S. Warr, G.H. Jacques, and J.M. Huntley, Powder Technol. **81**, 41 (1994).
[11] F. Melo, P. Ubanhovar, and H. Swinney, Phys. Rev. Lett. **72**, 172 (1994); **75**, 3838 (1995).
[12] M. Faraday, Philos. Trans. R. Soc. **52**, 299 (1831).
[13] M.C. Croos and P.C. Hohenberg, Rev. Mod. Phys. **65**, 851, (1993).
[14] S. Luding, H.J. Herrmann, and A. Blumen, Phys. Rev. E **50**, 3100 (1994).
[15] S. MacNamara and W.R. Young, Phys. Fluids A **5**, 34 (1993); B. Bernu, F. Delyon, and R. Mazighi, Phys. Rev. E **50**, 4551 (1994).
[16] P. Pieranski, J. Phys. (Paris) 44, 573 (1983); Phys. Rev. A **37**, 1782 (1988); A. Mehta and J.M. Luck, Phys. Rev. E **48**, 3988 (1993).
[17] Quantitative analysis of the patterns of Ref. [4] by C. Wassgreen, S. Gosh, and C.E. Breenen (unpublished).
[18] L.Vanel, E. Clément, J. Rajchenbach, and J. Duran (unpublished).
[19] A. Goldsthein, M. Shapiro, L. Moldavsky, and M. Fichman, J. Fluid. Mech., **287**, 349 (1995).
[20] L.D. Landau and E.M. Lifschitz, *Fluid Mechanics* (Pergamon Press, London, 1963).

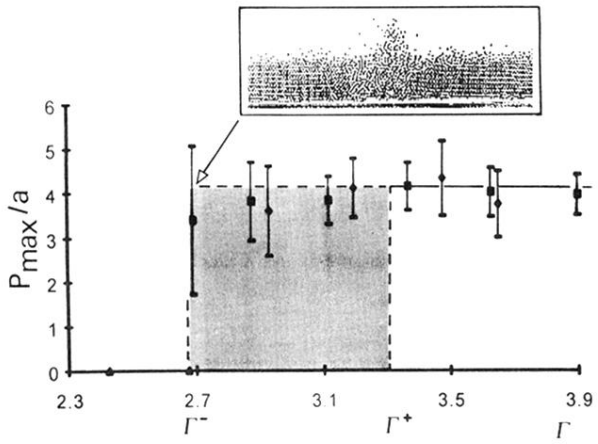

FIG. 5. Instability onset $P_{\max}/a$ as a function of the acceleration Γ: $a = 58$ mm (•) and $a = 48$ mm (♦).